

Experimental and Numerical Study on RC Frame Joint Strengthened with Enveloped Steel Plates

D. G. Weng, C. Zhang, J. D. Xia, X. L. Lu

State Key Laboratory for Disaster Reduction in Civil Engineering, Tongji University, China

S. M. Zhang

Department of Civil Engineering, Tongji University, China



15 WCEE
LISBOA 2012

SUMMARY:

The design principle of Strong Beam-Column Joints is essential for building structure to resist earthquakes, however, the recent field investigations show that joints in RC frame are susceptible to damage in the earthquake, and actually it is rather difficult and complicated to repair or strengthen these RC frame joints, thus research on seismic retrofit strategies for such joints is urgently required. A steel-enveloped approach to seismic retrofit of RC frame joints is proposed in this paper, while the pseudo static experimental research and the corresponding numerical modelling by FEM software ABAQUS are conducted to demonstrate its feasibility and validity. The test results and simulation results both indicate that the stiffness, bearing capacity and integrity of the steel-enveloped frame joint are significantly improved compared to the primary frame joint, while these parameters are also found to be directly related to the depth and covering size of the enveloped steel plates. Moreover, based on the comparative research of seismic performances of the frame joints before and after reinforcement, it is concluded that the steel-enveloped approach not only can be used to repair or strengthen the earthquake-damaged or existing RC frame joint for acquiring certain seismic performances, but also can be applied in damped RC frame structure to ensure the seismic safety of beam-column joints with additional dampers or steel braces.

Keywords: Beam-column joint; seismic retrofit; repair; enveloped steel; earthquake damage

1. INTRODUCTION

In designing an Ordinary Moment Resisting Frame (OMRF), often the seismic concepts of weak-beam strong-column and strong beam-column joint are implemented to ensure the damage mitigation and collapse prevention. However, according to the field investigation of recent destructive earthquakes, damages with weak-column strong-beam mode, as well as damage in beam-column joint, were rather common among RC frame damages, as shown in Figure 1.1. Other than the damaged frame joints, with the upgrade of seismic design codes (e.g. Chinese code for seismic design of buildings was revised after 2008 Wenchuan earthquake), the current seismic capacities of some existing RC frame joints might be not enough to meet their new requirements. Under this circumstance, it is necessary to do research on seismic repair or retrofit strategy for such damaged or existing RC frame joints. Furthermore, as to the RC frames retrofitted by using energy dissipation devices, the corresponding beam-column joints connected with dampers or braces are also needed to be strengthened additionally.



Figure 1.1. Damages of RC beam-column joint in the earthquake

Pursuant to this, a series of seismic retrofit strategies were proposed and developed to repair or strengthen the RC frame joints in the past, such as enlarging concrete section method, bonding steel method, gluing Fibreglass Reinforced Plastics (FRP) method, sticking Carbon Fibre Reinforced

Plastics (CFRP) method, etc. While the corresponding experimental and numerical investigations were conducted recently by many researchers (Tsonos 2008, Kam and Pampanin 2009, Pimanmas and Chaimahawan 2010, Yen and Chien 2010, Sadowski et al. 2010, Niroomandi et al. 2010, Mahini and Ronagh 2010, Le-Trung et al. 2010, Mahini and Ronagh 2011, Al-Zubaidy et al. 2012) to validate above methods [1-10]. Moreover, towards a RC frame retrofitted by viscous dampers, Weng and Zhang proposed a steel-enveloped approach to strengthen those frame joints which were connected with viscous dampers and braces (Weng et al. 2011, Zhang et al. 2011) [11-12], and also conducted a quasi-static test to validate the feasibility of this approach to repair damaged frame joints (Zhang et al. 2012) [13]. Subsequently, in this paper, other than experimental validation, the corresponding numerical analysis to the steel-enveloped approach was further conducted, so as to specify the design parameters and then study their different influences on practical retrofit effect, actually which were also demonstrated and compared with the test results.

2. STEEL-ENVELOPED APPROACH

The steel-enveloped approach proposed in this paper is to repair or strengthen the RC frame joint with enveloped steel plates throughout the floor slab, while break reinforcing bars in the floor slab around beam-column joint will be welded to the enveloped steel plates for reconnection, as shown in Figure 2.1, here the cover length of added steel plates on column is longer than that on beam, so that the post-retrofit joint area is of weak-beam strong-column. It is also noted that the gaps between internal beam-column joint and external steel jacket shall be filled with free grouting material or structural adhesive in light of practical design requirements. Mainly, the constructing process of this steel-enveloped approach contains the following four steps: (1) knocking off the broken concrete and cleaning the surfaces of beam-column joint; (2) cladding steel plates around the beam-column joint and welding them to a whole steel jacket; (3) sealing the gaps between internal frame joint and external steel jacket with different filler; (4) maintaining within the curing period, which is usually 28 days for non-shrinkage cement-based grouting material, and 14 days for structural adhesive.

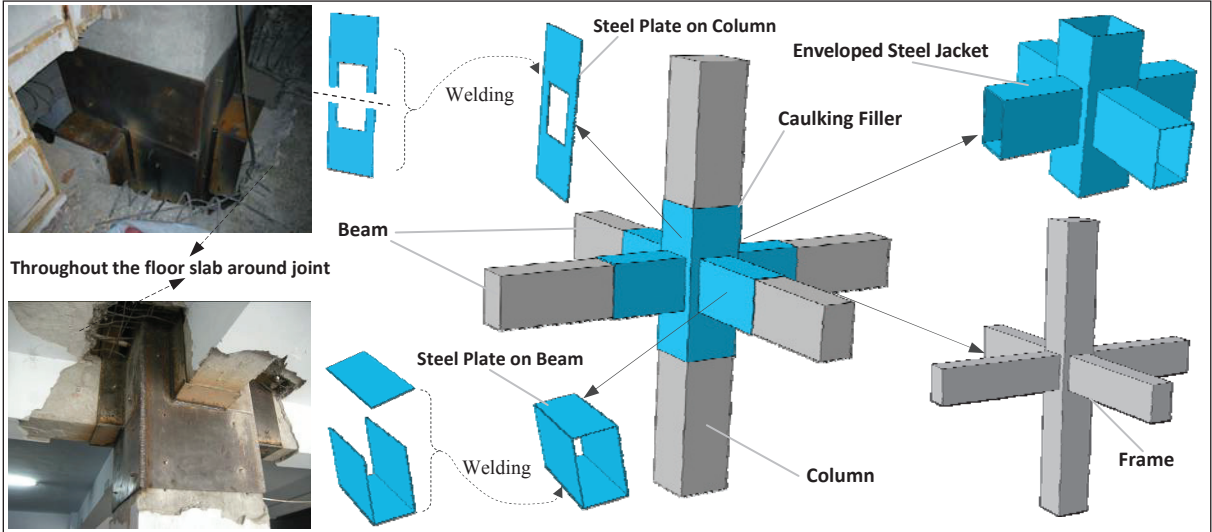


Figure 2.1. Structural details of steel-enveloped frame joint

As to the steel-enveloped approach, the key points are the parameter design of added steel jacket and the interface disposal measures to gaps, here these design parameters are determined based on the following two preconditions: (1) the original beam-column joint and the added steel jacket are both in elastic state; (2) the interior beam-column joint and the exterior steel jacket are not separated. Generally, design parameters of added steel jacket include the thickness and cover lengths on beam and column, respectively. In which, the cover lengths are usually determined with comprehensive consideration of the actual damage region and strength demand of beam-column joint, while the

thickness is mainly designed according to the requirements of bearing capacity (e.g. flexural capacity of beam section or shear capacity of column section). Moreover, it is also noteworthy that the strengthened beam-column joint with enveloped steel plates is a very limited area in the whole RC frame. Obviously, the corresponding beams and columns are divided into two parts after cladding enveloped steel plates, with or without steel jacket. While in practical design, bearing capacities of these two parts are required to satisfy their respective strength demands, and therefore design of added steel plates are conducted to shoulder the extra seismic effect (e.g. combination of bending moment, shear force, etc.) on beam and column, respectively.

However, according to the principle of weak-beam strong-column in frame, the beam is designed to be damaged before the column, and therefore it becomes a weak point in the earthquake. Thus the calculated thickness of steel plates added on beams shall be larger than that on columns in most case, but considering the construction convenience, the added steel plates on beams and columns are usually set the same thickness, that is, of course, the calculated thickness of steel plates added on the beam.

For instance, to make design of added steel plates on the beam, the real flexural capacity of the bare beam section and the steel-enveloped beam section can be calculated by Equations (2.1) ~ (2.3):

$$M_{y0} = \frac{1}{\gamma_{RE}} \cdot \left[f_{cm} \cdot b \cdot x \cdot \left(h_0 - \frac{x}{2} \right) + f_y' \cdot A_s' \cdot (h_0 - a_s') \right] \quad (2.1)$$

$$M_y = \alpha \cdot M_{y0} + \beta \cdot A_a \cdot f_{ay} \cdot h \quad (2.2)$$

$$f_{cm} \cdot b \cdot x = f_y \cdot A_s - f_y' \cdot A_s' \quad (2.3)$$

Where M_{y0} and M_y are real flexural capacity of the bare beam section and the steel-enveloped beam section, respectively; γ_{RE} is seismic adjusting factor for loading-bearing capacity of structural members; f_{cm} is combination value of bending-compression strength for beam, f_{ay} is combination value of tensile yield strength for added steel plate; f_y and f_y' are combination values of yield strength for tension and compression reinforcing bars, respectively; α is degradation effect factor with the consideration of structural damage, β is combination coefficient of added flexural capacity provided by steel jacket; x is relative height of equivalent compression zone, b and h are width and height of the beam, h_0 is the effective height; a_s' is concrete protective thickness of compression zone; A_s , A_s' , A_a are the sectional area of tension steel bars, compression steel bars and enveloped steel plates, respectively.

Supposed that the maximum bending moment on beam section with or without steel jacket is assigned to M_a and M_0 , respectively, thus to concord the maximum bending moments with the corresponding flexural capacities, the sectional area of added steel jacket can be calculated based on Equation (2.4):

$$A_a = \frac{\alpha \cdot M_{y0} \cdot (M_a - M_0)}{\beta \cdot f_{ay} \cdot h \cdot M_0} \quad (2.4)$$

Likewise, for the design of added steel plates on the column, similar design process can be conducted based on the balance of shearing force and shearing capacity in different column sections. Here it is noteworthy that the grouting hole and vent hole on the added steel jacket shall be reserved in advance, while the process of roughing surface and making slope shall also be conducted firstly on top surface of the original beams, so that the grouting material or structural adhesive can be smoothly filled up all the gaps in field construction stage.

3. EXPERIMENTAL INVESTIGATION

To validate the feasibility of this steel-enveloped approach, a pseudo-static test to three selected RC beam-column joint specimens was conducted. Here the experimental program contained the following three stages: pre-damage stage (i.e. to simulate the real earthquake damages), steel-enveloped retrofit stage, and reloading stage, while the selected three specimens were named as J1-1, J1-4 and J2-2. For brevity, this paper presented selected experimental results here, while further details of specimens and test process were available in reference of [13].

3.1. Specimen details and test setup

Figure 3.1 shows the dimensions and reinforcement details of J1-1, J1-4 and J2-2 specimens. Here the dimensions of beam and column were $250\text{mm}\times 400\text{mm}$ and $400\text{mm}\times 400\text{mm}$, respectively. The main and transverse reinforcements were deformed bars and plain mild steel, with different diameters as shown in Figure 3. It is noteworthy that the little differences among above three specimens are the main reinforcements in beam and the reinforcing bars in joint core area. To be specific, in the beam, four deformed bars with 20mm diameter are used for J1-1 and J2-2, and three deformed bars with 25mm diameter for J1-4; while in the joint core area, four additional deformed bars with 12mm diameter are applied only in J2-2 specimen, like the X-shaped reinforcing bars seen in Figure 3.1.

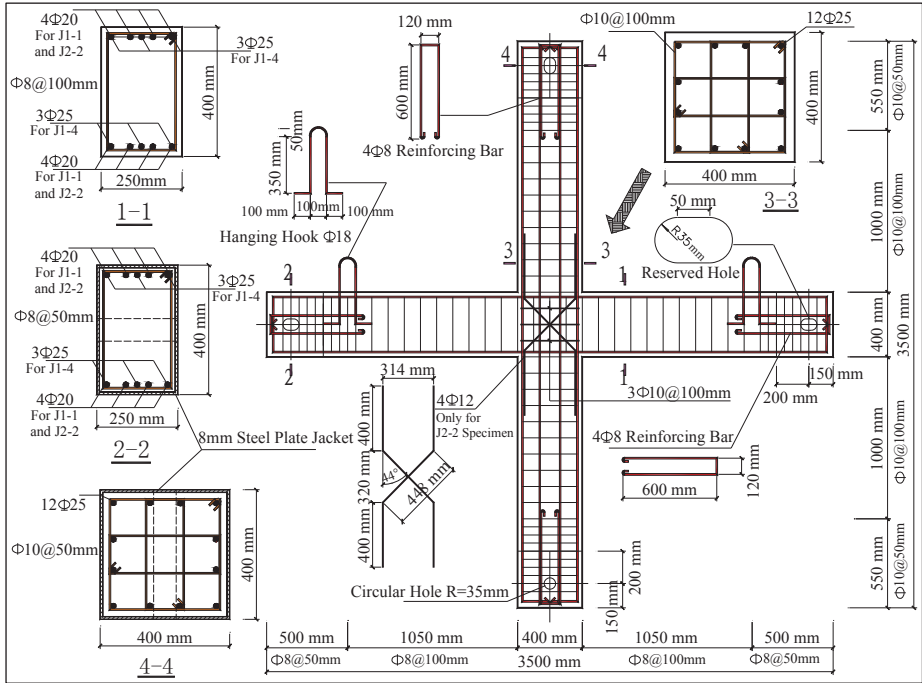


Figure 3.1. Information of J1-1, J1-4 and J2-2 specimens

Since the damaged joint ranges of the selected three specimens in this paper are similar, the cover length of added steel plates along beam and column direction are set to the same value for all the three specimens, and therefore the retrofiting programs are made based on different thickness of enveloped steel plates and different interface disposal measures, as listed in Table 3.1.

Table 3.1. Steel-enveloped program for J1-1, J1-4 and J2-2

Specimens	Cover Length of Steel Plates		Thickness of Steel Plate	Interface Disposal Measures
	Beam direction	Column direction		
J1-1	600 mm	400 mm	8 mm	Non-shrink Cement
J1-4	600 mm	400 mm	8 mm	Structural Adhesive
J2-2	600 mm	400 mm	5 mm	Non-shrink Cement

Noted: here the enveloped steel plate used in this paper adopts Q235 steel.

Figure 3.2 shows the testing setup. In this experiment, the planar beam-column specimen was framed by a free steel mechanism at its four ends of beam and column, respectively. Here the footing girder of the mechanism was fixed in the base by four bolts and the bottom end of column was hinged on this girder. The both ends of beam were tied to the mechanism by two hinge supports that allowed free horizontal movement to simulate the lateral drift. Moreover, to represent existing gravity load on the column, the axial load was vertically applied to the top end of the column by a hydraulic jack with 200 kN. Besides, a 1000 kN hydraulic actuator was attached to the upper girder of the steel mechanism, and the column was pushed and pulled at the top end with incremental displacements, which were controlled by the hydraulic actuator. Figure 3.3 illustrated the displacement-based loading scheme in this test. Here it is also noteworthy that the principle of loading scheme is one loop per loading step before the yield point and three loops per loading step after the yield point.

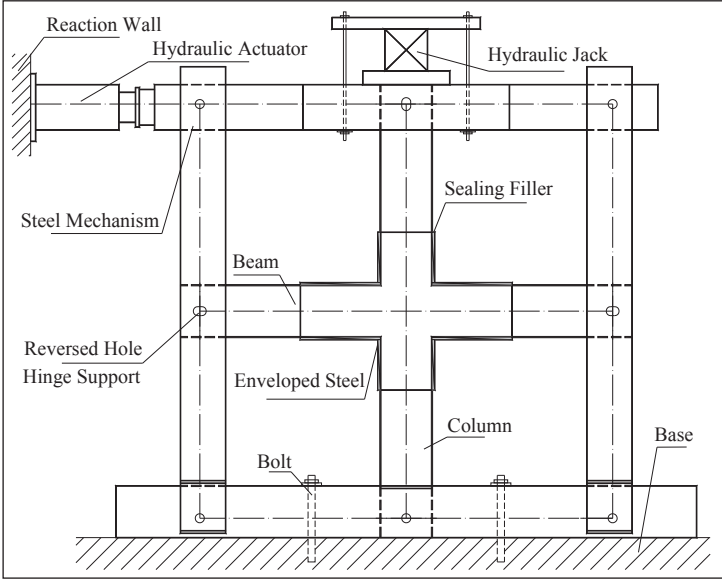


Figure 3.2. Testing setup

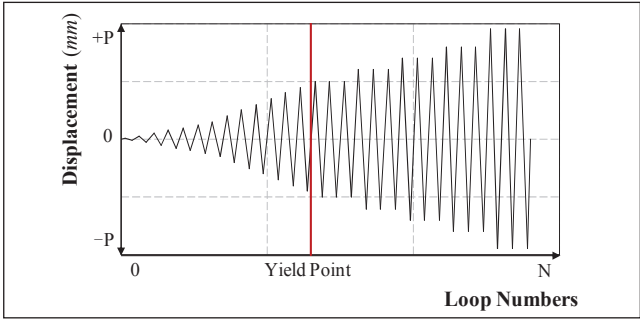


Figure 3.3. Displacement-based loading schemes

3.2. Test result and discussion

The comparative analysis of test results between pre-damage specimens and post-retrofit specimens were conducted for J1-1, J1-4 and J2-2, which referred to different hysteretic load-displacement relationship, skeleton-frame curves and failure patterns.

3.2.1. Hysteretic load-displacement relationship

Hysteresis curves presenting the relationship of lateral loads versus column top displacements for each specimen are shown in Figure 3.4. Here “Original” and “Retrofit” refer to the pre-damage specimen and post-retrofit specimen, respectively. From Figure 3.4, it can be obviously seen that yield strength and

yield displacement of all post-retrofit specimens are significantly increased, compared with original specimens. And it can also be concluded that the thickness of added steel jacket plays a more active role in increasing yield strength and ultimate strength of specimens, while different interface disposal measures do not. On the other hand, the hysteretic loops of original specimens is somewhat fuller than post-retrofit specimens under the same lateral loads, which indicates that the original specimen shoulder more seismic energy. But unfortunately, these energies are dissipated at the cost of more damages in the joint area, and this is, of course, not what people expected in practical seismic design.

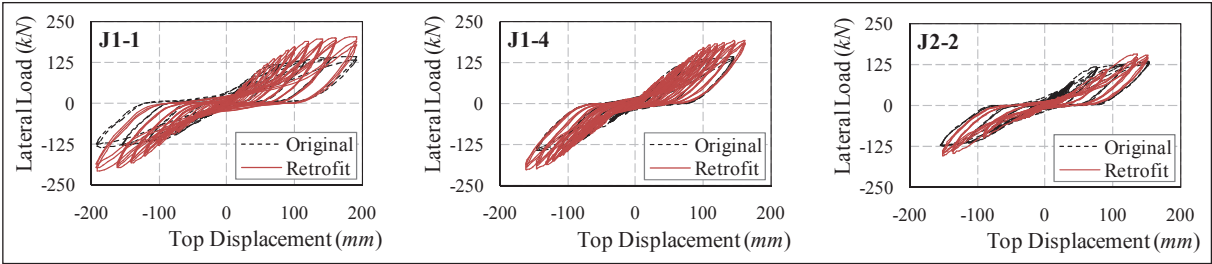


Figure 3.4. Relationship of lateral load versus top displacement

3.2.2. Hysteretic load-displacement relationship

Figure 3.5 shows the skeleton-frame curve for each specimen, which can not only well illustrate the change rule of yield strength and ultimate strength for all specimens before and after retrofit, but also indicate that the steel-enveloped approach has little influence on the initial stiffness of specimens. To be specific, as monitored at the loading position, the yield strength and ultimate strength of the pre-damaged specimens are about 117 kN and 140 kN, respectively, while the yield strength is increased to about 172 kN, 169 kN and 142 kN for post-retrofit J1-1, J1-4 and J2-2 specimens. Moreover, the ultimate strength of post-retrofit J1-1 and J1-4 specimens is estimated to more than 200 kN, and about 160 kN for J2-2 specimen. Obviously, the yield strength and ultimate strength of post-retrofit J1-1 and J1-4 are much larger than those of post-retrofit J2-2, in that the thickness of added steel jacket for J1-1 and J1-4 specimens are both 8 mm, but 5 mm for J2-2 specimen. Another reason for this phenomenon is probably attributed to severer damages in pre-damaged J2-2 specimen, which will result in a greater degradation of the stiffness and strength.

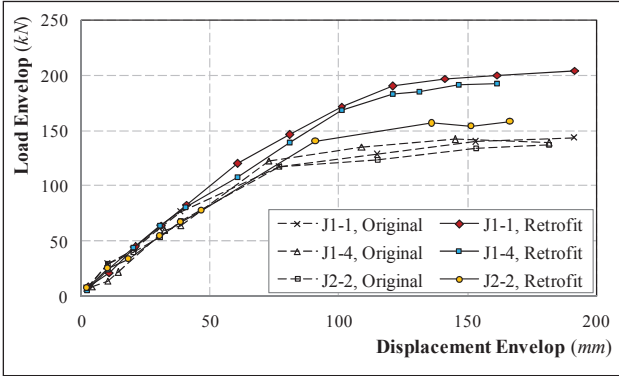


Figure 3.5. Load envelop versus displacement envelop

3.2.3. Failure pattern of specimens

Figure 3.6 shows the photos of all specimens after pre-damage test and reloading test. For original specimens (Figure 3.6a, 3.6b and 3.6c), a lot of cracks appeared on beams, columns and joint areas under incremental cyclic loading. However, there were little damages in post-retrofit specimens under approximately the same displacement loading cases, as shown in Figure 8d, 8e and 8f. Actually, for post-retrofit specimens, the joint areas were effectively strengthened by steel jackets and therefore performed well in reloading test. But the else parts of the specimen were reserved without any reinforcement measures, which resulted in some damages in the test, particularly on the beam surfaces

beyond the cover range of added steel jacket, cracks were expanded from the existing micro fractures in pre-damage loading stage. Thus, as to the whole specimen, although ultimate strength and ultimate displacement cannot be exactly tested due to aforementioned limitation of the hydraulic actuator, it can also be concluded that this steel-enveloped approach to seismic retrofit of beam-column joint is effective. However, these enhancements won't be unlimitedly increased, because when the strength of joint area is improved to a certain degree, the capacities of else parts will become the crucial factor in behavior of post-retrofit specimen under incremental cyclic loading.

To further explore the effect of different interface disposal measures, the added steel jacket of each specimen was cut open after the test, as shown in Figure 3.7. Here J1-1 and J2-2 specimens used non-shrink cement grouting material to seal the gaps, while J1-4 specimen used the structural adhesive. It can be obviously seen that the non-shrink cement grouting materials used in J1-1 and J2-2 specimens were gradually separated from the added steel jacket in the test, as shown in Figure 3.7a and 3.7c, while the structural adhesive used in J1-4 specimen tightly connected the added steel jacket and the damaged joint together into a whole, which was hardly separated after the test, as shown in Figure 3.7b. In fact, for J1-1 and J2-2 specimens, it was found to be empty through striking the steel jacket when loading to a certain displacement in the test. But for J1-4 specimen, there is not any empty between the added steel jacket and the internal damaged joint throughout the test.

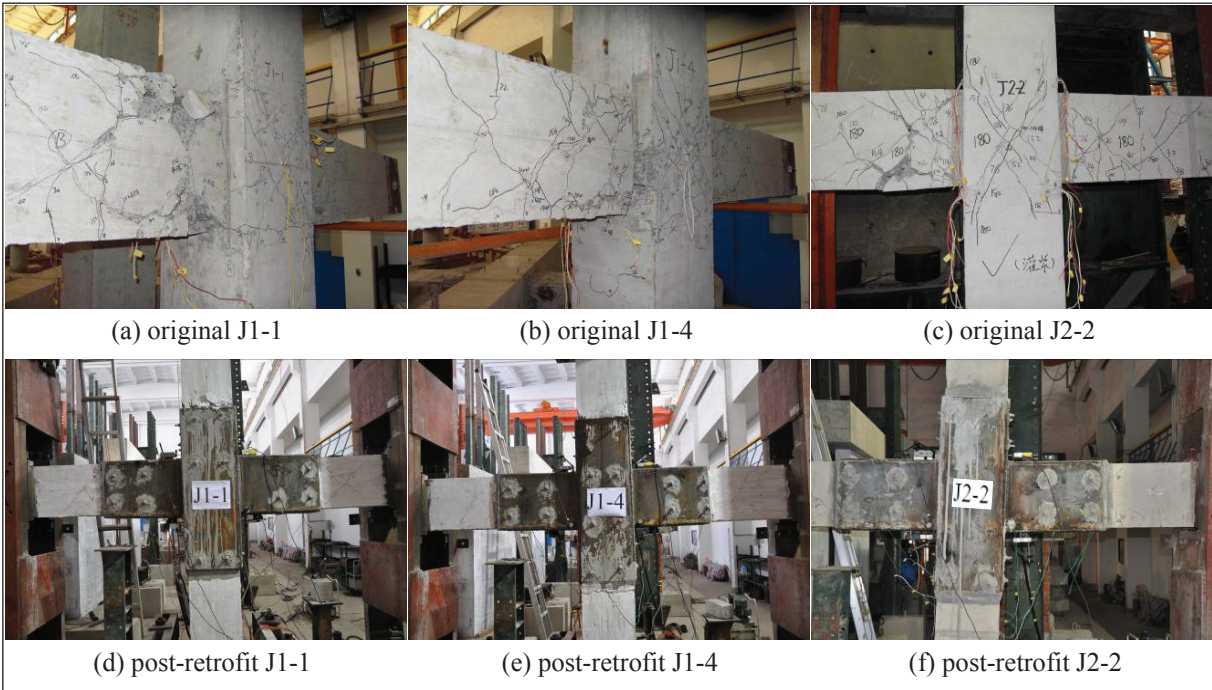


Figure 3.6. Photos of specimens after test



Figure 3.7. Damages of interface filler after cutting the enveloped steel jacket

4. NUMERICAL INVESTIGATION

The finite element models of selected test specimens are presented based on ABAQUS software, so as to make comparison with test results, and also to carry out parametric study on design of added steel jacket for this steel-enveloped approach. Herein the concrete is modeled using a solid element named C3D8R (i.e. Continuum, 3-Dimensional, 8-nodes, Reduced integration), while all steel bars and stirrups using a truss element named T3D2 (i.e. Truss, 3-Dimensional, 2-nodes), and the steel plates using shell element named S4R (i.e. Shell, 4-nodes, Reduced integration). The bilinear kinematic hardening (BKIN) model in ABAQUS is used to model the stress-strain curve of steel material (i.e. steel bars and steel plates), here the Bauschinger effect is taken into account, while the stiffness degradation is neglected during cyclic loading and the elastic modulus of steel material is supposed to be one percent of initial elastic modulus after yielding. Moreover, the concrete material is modelled by using concrete damaged plasticity model in ABAQUS, which uses concepts of isotropic damaged elasticity in combination with isotropic tensile and compressive plasticity to represent the inelastic behaviour of concrete. Based on [14~16], this model for concrete is of some macroscopic properties, such as different yield strengths in tension and compression, softening behaviour in tension as opposed to initial hardening followed by softening in compression, different degradation of the elastic stiffness in tension and compression, stiffness recovery effects during cyclic loading, etc. As to this concrete damaged plasticity model, the degraded response of concrete is characterized by two damage variables, which can be calculated by Equations (4.1) ~ (4.3), with the reference to [17].

$$d_k = \frac{(1-\beta) \cdot \varepsilon^{in} \cdot E_0}{\sigma_k + (1-\beta) \cdot \varepsilon^{in} \cdot E_0}, \quad (k = t, c) \quad (4.1)$$

$$\beta = \varepsilon^{pl} / \varepsilon^{in} \quad (4.2)$$

$$\varepsilon^{in} = \varepsilon - \sigma_k \cdot E_0^{-1}, \quad (k = t, c) \quad (4.3)$$

Where d_k is the damage variable, which refers to the tensile damage variable d_t and the compressive damage variable d_c ; β is the ratio of plastic strain to inelastic strain, while ε^{pl} is the plastic strain and ε^{in} is the inelastic strain; ε is the strain of concrete, σ_k is the stress correspond to (t represent to tension, c represent to compression); E_0 is the initial elastic modulus of concrete.

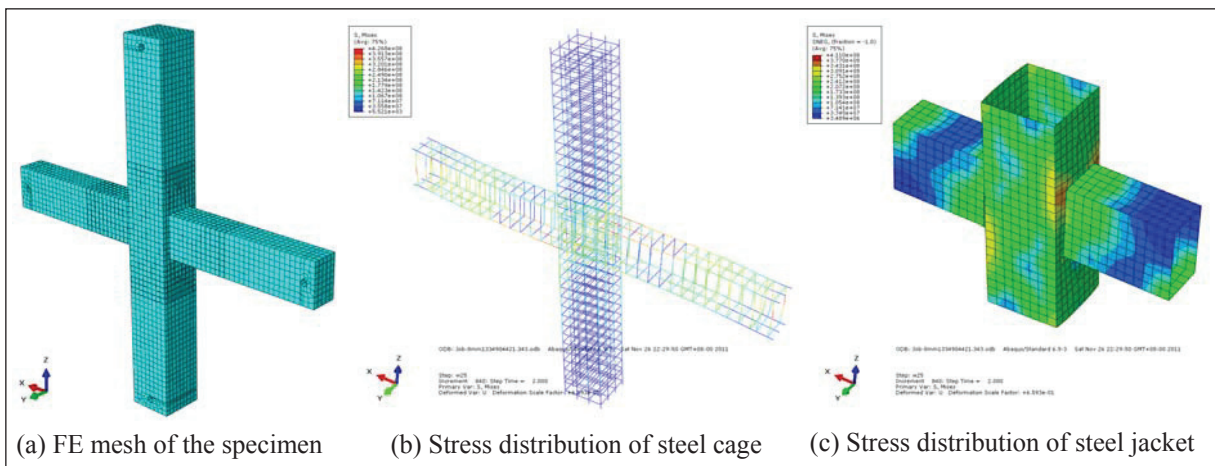


Figure 4.1. FE model of the post-retrofit specimen

Based on above simulating instructions, the finite element (FE) models of post-retrofit specimens are established, as shown in Figure 4.1, so as to conduct comparative demonstration with test results. In practice, since experimental program for three test specimens (i.e. J1-1, J1-4 and J2-2) is similar, the

parametrical study here only chooses the post-retrofit specimen of J1-4 for instance to prepare FE model and carry out numerical investigation. Figure 4.1a shows the FE mesh of the selected specimen (i.e. J1-4), Figure 4.1b ~ 4.1c show the stress distribution of steel cages and steel jacket, respectively. From above Figures, it is obvious that the beam in this specimen is weaker than the column, and therefore stress and deformation on the beam are relatively larger than those on the column.

As mentioned in Section 2, design parameters of added steel jacket generally include the thickness, the cover lengths on beam and on column, which are marked as t , L_b and L_c , respectively, as shown in Figure 4.2. With the combination of test result of post-retrofit J1-4 specimen (i.e. $t=8mm$, $L_b=600mm$, $L_c=400mm$), the load-displacement curves at the load point (i.e. Top column of the specimen) with different thickness of added steel jacket (i.e. $t=2mm$, $5mm$, $8mm$, $10mm$, $15mm$, $20mm$) are shown in Figure 4.2a, here supposed that $L_b=600mm$, $L_c=400mm$. Likewise, Figure 4.2b shows the load-displacement curve with different cover length on beam ($L_b=100mm$, $200mm$, $300mm$, $400mm$, $500mm$, $600mm$), supposed that $t=8mm$, $L_c=400mm$; Figure 4.2c shows the load-displacement curve with different cover length on column ($L_c=100mm$, $200mm$, $300mm$, $400mm$), supposed that $t=8mm$, $L_b=600mm$. Based on Figure 4.2, it can be easily seen that the thickness of added steel jacket plays a great role in increasing the yield strength and the initial stiffness of the specimen, while the cover length on beam only affects strength index, but the cover length on column has little impact on both the yield strength and the initial stiffness of the specimen. Here it is also noteworthy that the same corollary can be obtained through aforementioned experimental investigation.

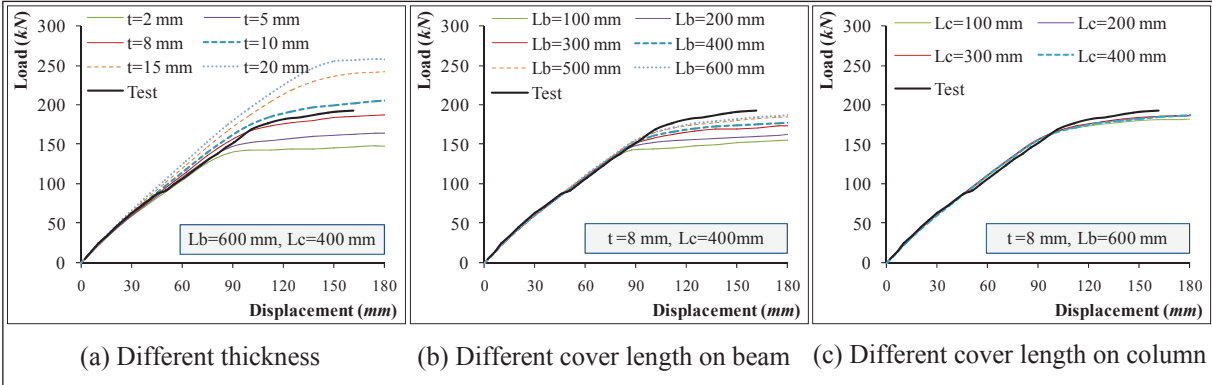


Figure 4.2. Numerical results with different design parameters of added steel plates

Since the cover length of added steel jacket on beam and column are relatively not sensitive to loading behavior of the specimen, here more attention is paid to further study on the thickness of added steel jacket. Based on above simulation result, it is concluded that the yield strength of the specimen is apparently improved with the increase of the thickness. Both the theoretical calculation (i.e. in Section 2) and the test result (i.e. in Section 3) support this conclusion. However, the increase of yield strength won't be prolonged indefinitely with the increasing thickness, in that the parts without added steel jacket of the specimen will be the determining factor in seismic design or loading process. As depicted by Wooden Barrel theory, each cask will always be a piece of board as soon as possible, and therefore the bucket of water storage depends on the shortest board level. So does seismic retrofit of frame joint, it is unnecessary to strengthen the joint area too much stronger than other bare parts.

5. CONCLUDING REMARKS

The test results reported herein and the numerical investigation have led to the following conclusions concerning this steel-enveloped approach to strengthening of frame joint:

The thickness of added steel jacket plays a more active role in increasing the yield strength and ultimate strength of original specimens while different interface disposal measures do not. However,

regardless of different thickness and different interface disposal measures, the initial stiffness of post-retrofit specimens is rarely improved compared to that of original specimens. Moreover, the cover length of added steel jacket on beam only affects strength index, but the cover length on column has little impact on both the yield strength and the initial stiffness of the specimen.

Due to the restriction from else parts of the specimen beyond the cover range of added steel jacket, it is rather pointless to excessively reinforce the damaged beam-column joint. Actually, when the beam-column joint is strengthened to a certain level, the seismic capacity of the whole specimen is not decided by the joint core area, but up to the capacity of the else bare parts.

As to the interface disposal measures, the structural adhesive is evidently better than the cement-based grouting material to connect the internal beam-column joint and external steel jacket as a whole, but with more expensive price and poorer durability. Accordingly, considering the economy and convenience to construction, the cement-based grouting material is more commonly used in practice.

ACKNOWLEDGEMENT

The authors wish to gratefully acknowledge the generous support of this work by the National Key Technology R&D Program of China under Grant No. 2009BAJ28B02 and the Key Consulting & Research Project of Chinese of Academy Engineering under Grant No. 2010-ZD-4, and also extend special thanks to Sen Li and Linhai Peng, for their experimental data and analysis work.

REFERENCES

- [1] Tsonos, A. G. (2008). Effectiveness of CFRP-jackets and RC-jackets in post-earthquake and pre-earthquake retrofitting of beam-column subassemblages. *Engineering Structures*. **30:3**, 777-793.
- [2] Kam, W.Y. and Pampanin, S. (2009). Experimental and Numerical Validation of Selective Weakening Retrofit for Existing Non-Ductile R.C. Frames. *Improving the Seismic Performance of Existing Buildings and Other Structures*. **Vol I**: S7-2.
- [3] Pimanmas, A. and Chaimahawan, P. (2010). Shear strength of beam-column joint with enlarged joint area. *Engineering Structures*. **32:9**, 2529-2545.
- [4] Yen, J. Y. R. and Chien, H. K. (2010). Steel plates rehabilitated RC beam-column joints subjected to vertical cyclic loads. *Construction and Building Materials*. **24:3**, 332-339.
- [5] Sadowski, T., Kneć, M., and Golewski, P. (2010). Experimental investigations and numerical modeling of steel adhesive joints reinforced by rivets. *International Journal of Adhesion & Adhesives*. **30:5**, 338-346.
- [6] Niroomandi, A., Maheri, A., Maheri, M. R., et al. (2010). Seismic performance of ordinary RC frames retrofitted at joints by FRP sheets. *Engineering Structures*. **32:8**, 2326-2336.
- [7] Mahini, S. S. and Ronagh, H. R. (2010). Strength and ductility of FRP web-bonded RC beams for the assessment of retrofitted beam-column joints. *Composite Structures*. **9:6**, 1325-1332.
- [8] Le-Trung, K., Lee, K., Lee, J., et al. (2010). Experimental study of RC beam-column joints strengthened using CFRP composites. *Composites Part B: Engineering*. **41:1**, 76-85.
- [9] Mahini, S.S. and Ronagh, H.R. (2011). Web-bonded FRPs for relocation of plastic hinges away from the column face in exterior RC joints. *Composite Structures*. **93:10**, 2460-2472.
- [10] Al-Zubaidy, H., Al-Mahaidi, R., and Zhao, X. L. (2012). Experimental investigation of bond characteristics between CFRP fabrics and steel plate joints under impact tensile loads. *Composite Structures*. **94:2**, 510-518.
- [11] Weng, D. G., Zhang, C., and Lu, X. L. (2011). Application of Energy Dissipation Technology to C-category Frame Structure of School Buildings for Seismic Retrofit of Increasing Precautionary Intensity. *Journal of Advanced Materials Research*. **163-167**, 3480-3487.
- [12] Zhang, C., Weng, D. G., and Lu, X. L. (2011). A Simplified Design Method for Energy-dissipated Structure with Viscous Dampers. *Proceeding of 8CUEE Conference*. **Vol I**: 1335-1343.
- [13] Zhang, C., Weng D. G., Xia, J. D., et al. (2012). Experimental Research on Seismic Behavior of Post-retrofit Earthquake-damaged Frame Joint. *Proceeding of 9CUEE and 4ACEE Conference*. **Vol I**: 893-900.
- [14] Lubliner, J., Oliver, J., Oller, S., Oñate, E. (1989). A plastic-damage model for concrete. *International Journal of Solids and Structures*. **25:3**, 299-326.
- [15] Lee, J., and Fenves, G. L. (1998). A plastic-damage model for cyclic loading of concrete structure. *Journal of Engineering Mechanical*. **124:8**, 892-900.
- [16] ABAQUS User Manual. ABAQUS, Inc, 2006
- [17] Birtel, V., and Mark, P. (2006). Parameterized finite element modeling of RC beam shear failure. *Proceeding of 2006 ABAQUS User's Conference*. **Vol I**: 95-108.